MICHIGAN STATE UNIVERSITY

CYCLOTRON LABORATORY

THE DISAPPEARANCE OF FUSION-LIKE RESIDUES AND THE NUCLEAR EQUATION OF STATE

H.M. XU, W.G. LYNCH, P. DANIELEWICZ,
and GEORGE BERTSCH

MAY 1990

MSUCL-724

The Disappearance of Fusion-like Residues and the Nuclear Equation of State

H.H. Xu, W.C. Lynch, P. Danielewicz and G.F. Bertsch

National Superconducting Cyclotron Laboratory and
the Department of Physics, Michigan State University
East Lansing, Michigan 48824.

Abstract

The cross sections for massive residues from $^{40}Ca + {}^{40}Ca$ and $^{40}Ar + {}^{27}Al$ collisions were calculated with a improved BUU equation. The calculated residue cross sections decrease with incident energy, an effect which does not appear related to the residue excitation energy. Larger residue cross sections result from calculations with larger in-medium nucleon-nucleon cross sections or with equations of state which are less attractive at sub-nuclear density. This dual sensitivity may be eliminated by measurements of observables associated with the coincident light particles,

PACS numbers:25.70.Jj, 25.70.Np

Hot nuclei can be readily formed by the incomplete fusion of projectile and target nuclei in a heavy ion reaction.[1-9] For moderate incident energies, the excitation energies of fusion-like residues increase with incident energy.[1,3,9] At incident energies in excess of about E/A ≈ 35-40 MeV, however, vanishing cross sections for fusion-like residues have been reported,[1,4-8] and interpreted[1,3,6,7,9] as a manifestation of a bulk instability of nuclei at high temperatures.[6,10,11] This interpretation may be unwarranted if very hot nuclei decay via unexpected decay modes,[12-14] or if the reaction dynamics preclude the formation of very highly excited residues.[2,15]

To investigate the dynamical limits to the formation of hot composite nuclei, heavy residue cross sections were calculated for $^{40}Ca + ^{40}Ca$ and $^{40}Ar + ^{27}Al$ collisions using the Boltzmann equation.[16] Qualitatively consistent with experimental observations,[1,4-8] the calculated heavy residue cross sections decrease rapidly to zero for E/A > 35-40 MeV. The decrease in cross section does not appear related to a bulk instability of nuclei at high temperature. The calculated cross sections are quite sensitive to the in-medium nucleon-nucleon cross section and the nuclear equation of state (EOS) at sub-nuclear density.

The calculations were performed by solving numerically the Boltzmann-Uehling-Uhlenbeck (BUU) equation which describes the time evolution of the Wigner-function $f(\vec{r},\vec{k},t)$ in phase space,[16]

$$\frac{\partial f_1}{\partial t} + \vec{v}\cdot\vec{\nabla}_r f_1 - \vec{\nabla}_r U\cdot\vec{\nabla}_p f_1 = \frac{4}{(2\pi)^3}\int d^3k_2 d\Omega \frac{d\sigma(\Omega)}{d\Omega}_{nn} v_{12}[f_3 f_4(1-f_1)(1-f_2) - f_1 f_2(1-f_3)(1-f_4)]. \quad (1)$$

Here, $\frac{d\sigma(\Omega)}{d\Omega}_{nn}$ and v_{12} are the in-medium cross section and relative velocity for the colliding nucleons, and U is the mean field potential consisting of the Coulomb potential and a nuclear potential with isoscaler and symmetry terms. For simplicity, $\frac{d\sigma(\Omega)}{d\Omega}_{nn}$ was chosen to be isotropic and energy independent.[17]

The isoscaler potential field U_o was approximated by

$$U_o(\rho) = -A\rho/\rho_o + B(\rho/\rho_o)^Y \quad \text{(MeV)}. \quad (2)$$

Values for A, B, and Y, given in Table 1, were used in specific calculations to provide soft (K=200 MeV) or stiff (K=375 MeV) equations of state. The symmetry potential, U_{sym}, was approximated by

$$U_{sym} = 32\,\frac{(\rho_n-\rho_p)}{\rho_o}\,\tau_z \quad \text{(MeV)}, \quad (3)$$

where ρ_n and ρ_p are the neutron and proton densities and τ_z is the isospin operator with eigenvalues +1 and -1 for neutrons and protons, respectively. Numerical solutions to Eq. 1 were obtained by propagating test particles on a potential grid according to Newtonian mechanics following the Lattice Hamiltonian method of Lenk and Pandharipande.[18] This method ensured energy

conservation to better than 0.1 MeV per nucleon over a time period of about 300 fm/c. The mean field and the Pauli blocking factors in the collision integral were averaged over an ensemble of 80 parallel simulations. For $A \geq 30$, nuclei bound by the soft EOS were in good agreement with the liquid drop mass formula.[19] For nuclei bound by the stiff EOS, the binding energy/nucleon of nuclei in this mass range was 0.4 - 0.8 MeV less than with the soft EOS, mainly because the surface energy coefficient for the stiff EOS was somewhat larger.

To illustrate the features of these calculations we consider calculations for $^{40}Ca + {}^{40}Ca$ system at E/A = 40 MeV. For this system, calculations were performed for an isotropic nucleon-nucleon cross section of $\sigma_{NN} = \int d\Omega \cdot \frac{d\sigma(\Omega)}{d\Omega} =$ 41 mb[17] and both soft and stiff equations of state. Fig. 1 shows the masses (upper left panel) and the component of velocity parallel to the beam axis (lower left panel) of heavy residues produced in the calculations. Two residues with $30 \leq A \leq 40$ are produced at large impact parameters $b > 3.3$ fm for calculations with the stiff EOS (open points) and the soft EOS (open squares). A single heavy residue is observed at small impact parameters, $b \leq 3.3$ fm, in calculations with the stiff EOS (solid points). For small impact parameters with the soft EOS, however, the projectile and target simply pass through each other, with their velocities and masses reduced. (More complicated multi-fragment final states are suppressed by the ensemble averaging of the mean field potential.) The total orbital angular momentum of the fusion-like residue produced in calculations with the stiff EOS (upper right panel) increases linearly with impact parameter to a value of about 60 $\hbar$ at $b \approx 3.3$ fm, comparable to the maximum orbital angular momentum predicted by

the liquid-drop model[20] for mass A≈60. This suggests that formation of a residue may be partially limited by angular momentum considerations.

The total excitation energy of the residues is shown at t = 120 fm/c by the solid points in the lower right hand panel in Fig. 1 for fusion-like residues produced in calculations with the stiff EOS. The total excitation energy increases slightly with impact parameter; this increase is partly due to the collective energy of rotation. The solid crosses depict the excitation energy after the rotational energy has been subtracted. To enable more accurate estimations of the thermal excitation of the residue, a collective velocity field was defined on the computational lattice,[21] and an integration was performed to obtain a total kinetic energy of collective motion. After subtracting the total collective energy, the intrinsic excitation energy, designated by the solid diamonds, decreases slightly with impact parameter. Thus in these dynamical calculations, the formation of heavy residues does not appear to be limited by the stability of the residual nucleus at high temperature. Indeed, in larger impact parameter collisions, where residue formation is tenuous, the intrinsic excitation energies are somewhat smaller.

The energy dependences of the heavy residue cross sections for calculations with soft and stiff equations of state are indicated respectively by the solid squares and solid points in the upper half of Fig. 2. Each symbol (square or point) is obtained from the largest calculated impact parameter which yields massive fusion-like residues; the upper edge of each vertical bar corresponds to the smallest calculated impact parameter which yields distinct projectile- and target-like residues. For a constant nucleon-nucleon cross

section of 41 mb, the cross sections for fusion-like residues are larger for calculations with the stiff EOS.

To see which part of the equation of state is responsible for the varying fusion cross sections, we performed calculations at E/A = 40 MeV with equations of state having variable low- and high-density behavior. For example, we define a soft-stiff equation of state which follows the soft EOS at low density and the stiff EOS at high density. The parameterizations for this and the analogous stiff-soft equation of state are given in Table I. The $^{40}Ca+^{40}Ca$ heavy residue cross sections obtained with these EOS's, 330±30 mb for stiff-soft and 120±20 mb for soft-stiff, show that the residue cross section depends mainly on the low density EOS.

This sensitivity to the low-density EOS could have been anticipated from the qualitative study of ref. 22. There it is shown that compression of nuclear matter in one-dimensional collisions is followed by a rarefaction, and the maximum tensile strength of the nuclear matter in the low-density phase depends on the EOS. Stiffer equations of state have higher tensile strengths, and so the tendency of the system to breakup into two or more fragments is less.

A possible determination of the low-density EOS on the basis of the cross sections for residue formation is hindered by the fact that these cross sections are also sensitive to σ_{NN}. To illustrate the possible theoretical ambiguities, calculations were performed for the $^{40}Ar+^{27}Al$ system in which the value for σ_{NN} was adjusted separately for calculations with both stiff and soft equations of state to obtain residue cross sections of about 500 mb at

E_{Lab}/A = 30 MeV. These choices, (1) σ_{NN} = 25 mb and a stiff EOS and (2) σ_{NN} =50 mb and a soft EOS, provide essentially equal residue cross sections at E/A ≤ 30 MeV. The energy dependence of the residue cross sections predicted by both calculations is qualitatively consistent with experimental observations.[6-7] Differences between the two sets of calculations at E_{Lab}/A > 30 MeV may not be large enough to discriminate between different equations of state. One must also assess the differences that could arise from variations in the energy dependence in the in-medium nucleon-nucleon cross section.

Measurements of additional observables may help to reduce these ambiguities. For example, the top panel in Fig. 3 shows the corresponding predictions for the ratio of the yield of nucleons emitted in the reaction plane over the yield emitted out of the reaction plane for center of mass angles, $30° \leq \theta_{c.m.} \leq 150°$, and energies, $E_{cm} \geq 20$ MeV . Calculations with the soft EOS and σ_{NN}=50 mb are more isotropic.[23] The greater isotropy of calculations with larger σ_{NN} is also manifested in the dependence of the mean transverse momentum of emitted nucleons upon rapidity, shown in the bottom panel of Fig. 3. Significantly larger transverse momenta are predicted at $Y < Y_{beam}$ for calculations with smaller values for σ_{NN}. Even larger anisotropies would be expected for deuterons, tritons or α particles within the coalescence approximation for cluster emission. Given advances in the treatment of cluster production, such large anisotropies in the emission of the heavier hydrogen and helium isotopes could provide significant constraints on σ_{NN} and consequently, on the EOS, if anisotropy measurements are combined with heavy residue cross sections.

Some caution must be exercised when comparing these residue cross sections to experimental data. Since these excited residues will decay, all residue decay channels, including the binary emission of heavy fragments,[12,24,25] must be experimentally measured and summed before comparisons to the calculated cross sections of Fig. 2 can be made. From the theoretical side, additional investigations are necessary to assess whether prompt multi-fragmentation processes,[26] not considered by the present Boltzmann code, remove flux from the reaction trajectories that lead to heavy residue formation in the present calculations. Investigations are also required to assess the sensitivity of the residue cross sections to details of the Pauli-blocking algorithm and details of the surface energies of the computational nuclei.

In summary, calculations have been performed with the Boltzmann equation to assess the sensitivity of heavy residue cross sections to the EOS and the in-medium nucleon-nucleon cross section. For specific choices of σ_{NN} and the nuclear EOS, the calculated residue cross sections decrease and eventually vanish for incident energies above E/A $\geq$ 35 MeV, consistent with experimental observations. This decrease in cross section does not seem to be related to a bulk instability of nuclei at high temperature. The calculated residue cross sections are sensitive to both the nuclear EOS and the nucleon-nucleon cross section. This dual sensitivity constitutes an ambiguity which may be reduced or eliminated by measurements of observables like the in/out-of-plane ratio and the mean transverse momentum that are related to the isotropy of the emission patterns of coincident light particles.

We would like to acknowledge many helpful and fruitful discussions with M. Tohyama, C.K. Gelbke and M.B. Tsang. This work was supported by the National Science Foundation under Grant Nos. PHY-86-11210, PHY-87-14432, and PHY-89-05933 and a NSF Presidential Young Investigator Award.

References

1. S. Leray, J. Phys. Colloq. 47 C4, 275 (1986).
2. J. Galin, Nucl. Phys. A488, 297c (1988).
3. D. Fabris, et al, A471, 351c (1987).
4. D. Jaquet, et al, Phys. Rev. Lett. 53, 2226 (1984).
5. E. Suraud, C. Grégoire, and B. Tamain, Prog. Part. Nucl. Phys., 23, 357 (1989).
6. G. Auger, et al, Phys. Lett. B 169, 161 (1986).
7. A. Fahli, Phys. Rev. C34, 161 (1986).
8. H. Nifenecker, et al, Nucl. Phys. A447, 533c (1985).
9 B. Bourderie and M.F. Rivet, Z. Phys. A321, 703 (1985.
10. S. Levit and P. Bonche, Nucl. Phys. A437, 426 (1984).
11. H. Sagawa, and G.F. Bertsch, Phys. Lett. B 155 11 (1985).
12. E. Plagnol, et al, Phys. Lett. B 221, 11 (1989).
13. D.H.E. Gross, Phys. Lett. B 203, 26 (1988).
14. J. Bondorf et al, Nucl. Phys. A443, 321 (1985).
15. S. Bhattacharya, Phys. Rev. Lett. 62, 2589 (1989).
16. G.F. Bertsch, H. Kruse, and S. Das Gupta, Phys. Rev. C29, (1984) 673; G.F. Bertsch, and S. Das Gupta, Phys. Rep. 160, (1988) 189, and references contained therein.
17. An isotropic energy independent cross section has been chosen solely for reasons of simplicity. In general, σ_{NN} is expected to be energy and density dependent.
18. R.J. Lenk and V.R. Panharipande, Phys. Rev. C39, (1989) 2242.
19. W.D. Myers and W.J. Swiatecki, Nucl. Phys. 81, 1 (1966); W.D. Myers and W.J. Swiatecki, Ann. Phys. 55, 186 (1969).

20. S. Cohen, F. Plasil, and W. J. Swiatecki, Ann. Phys. (New York) 82, 557 (1974).

21. B. Remaud, C. Gregoire, F. Sebille and P. Schuck, Nucl. Phys. A488, (1988) 423c.

22. G. Bertsch and D. Mundinger, Phys. Rev. C17,1646 (1978).

23. G.F. Bertsch, W.G.Lynch, and M.B. Tsang, Phys. Lett. B 189, (1987) 384; M.B. Tsang, G.F. Bertsch, W.G. Lynch and Mitsuru Tohyama, Phys. Rev. C40, (1989) 1685.

24. W.A. Friedman and W.G. Lynch, Phys. Rev. C28, 950 (1980).

25. L.G. Moretto, Phys. Lett. B 40, 185 (1972).

26. W. Bauer, et al, Phys. Rev. Lett. 58, 863 (1987)

Table 1. Mean Field Parameterizations

Set	Label	range	A(MeV)	B(MeV)	Y	K($\rho=\rho_o$)(MeV)
1	soft	$0<\rho/\rho_o<\infty$	356	303	7/6	200
2	stiff	$0<\rho/\rho_o<\infty$	124	70.5	2	375
3	soft-stiff	$\rho/\rho_o<1.024$	356	303	7/6	
		$1.024<\rho/\rho_o$	124	70.5	2	
4	stiff-soft	$\rho/\rho_o<1.024$	124	70.5	2	
		$1.024<\rho/\rho_o$	356	303	7/6	

Figure Captions

Fig. 1: Observables calculated for the $^{40}Ca+^{40}Ca$ system at E/A=40 MeV assuming σ_{NN}=41 mb. Upper left: Mean residue masses. Lower left: Component of the mean residue velocity parallel to the beam. Upper right: Mean residue angular momentum for the stiff EOS. Lower right: Mean residue total excitation energy/nucleon (solid points), after subtracting the rotational energy (crosses), and after subtracting the total collective energy (solid diamonds) for calculations with the stiff EOS. The lines are drawn to guide the eye.

Fig. 2: Upper half: Residue cross sections for $^{40}Ca+^{40}Ca$ collisions. The arrow indicates zero cross section for soft EOS. Lower half: Residue cross sections for $^{40}Ar+^{27}Al$ collisions. The solid points and solid squares describe calculations with the stiff and soft equations of state, respectively. The lines are drawn to guide the eye.

Fig. 3: In/out-of-plane ratios and mean transverse momenta for unbound nucleons with $E_{c.m.} \geq 20$ MeV from calculations for the $^{40}Ar+^{27}Al$ system at E/A = 30 MeV for σ_{NN}=25 mb with a stiff EOS (solid points) and σ_{NN}=50 mb with a soft EOS (solid squares). Upper half: Ratios of the nucleon yield in the reaction plane (azimuthal angles $-30° < \Phi < 30°$ and $150° < \Phi < 210°$) to the nucleon yield out of the reaction plane ($60° < \Phi < 120°$ and $240° < \Phi < 300°$) for the polar angles $30° \leq \theta_{cm} \leq 150°$. Lower half: The component of the mean transverse momentum of unbound nucleons in the reaction plane as a function of rapidity. A weighted sum over impact parameters b≤4 fm has been performed. The lines are drawn to guide the eye.

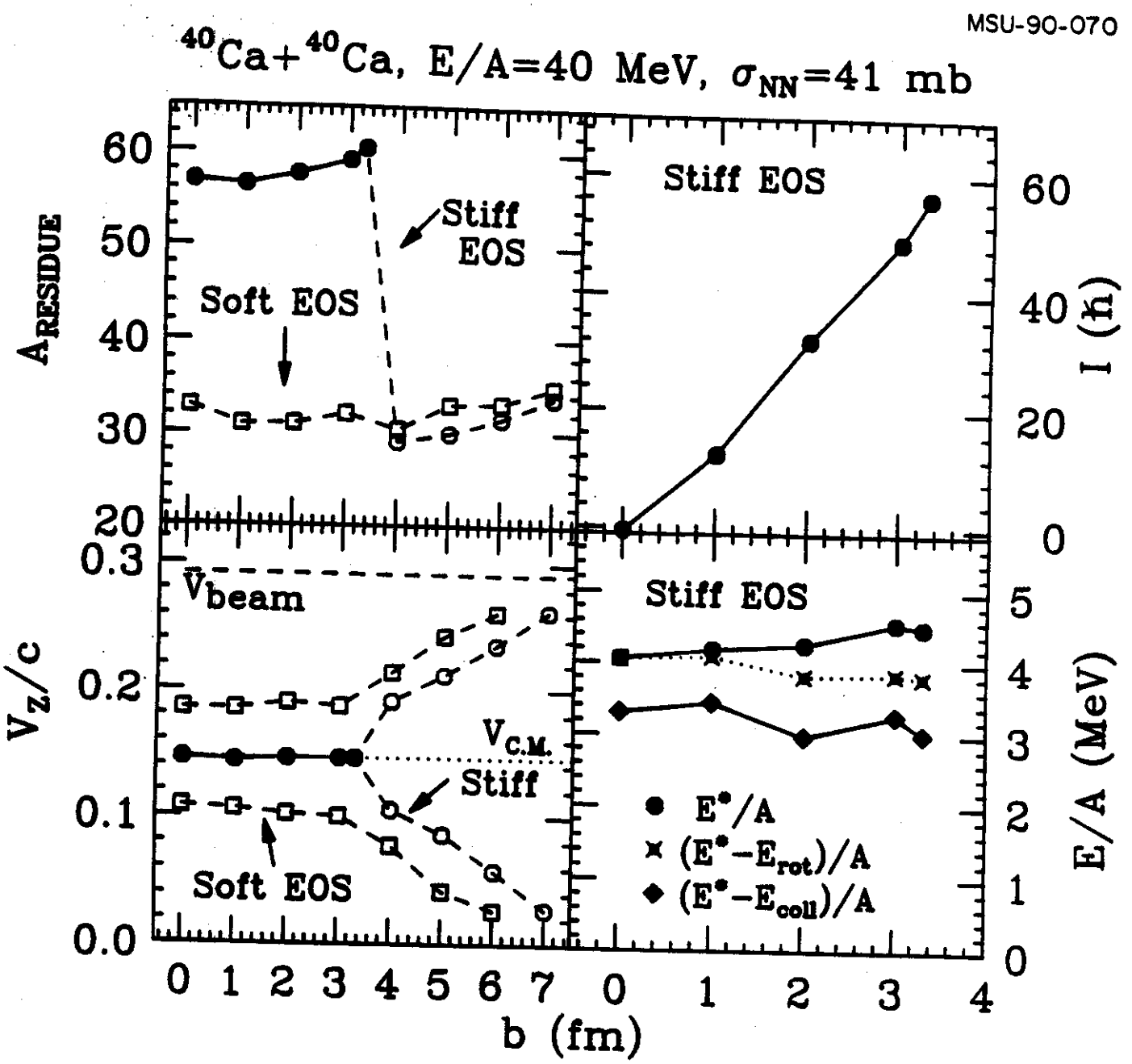
MSU-90-070
$^{40}Ca+^{40}Ca$, E/A=40 MeV, σ_{NN}=41 mb
$A_{RESIDUE}$
Stiff EOS
Soft EOS
Stiff EOS
I (ħ)
V_{beam}
$V_{C.M.}$
Stiff
Soft EOS
V_Z/c
Stiff EOS
E^*/A
$(E^*-E_{rot})/A$
$(E^*-E_{coll})/A$
E/A (MeV)
b (fm)

Fig. 1

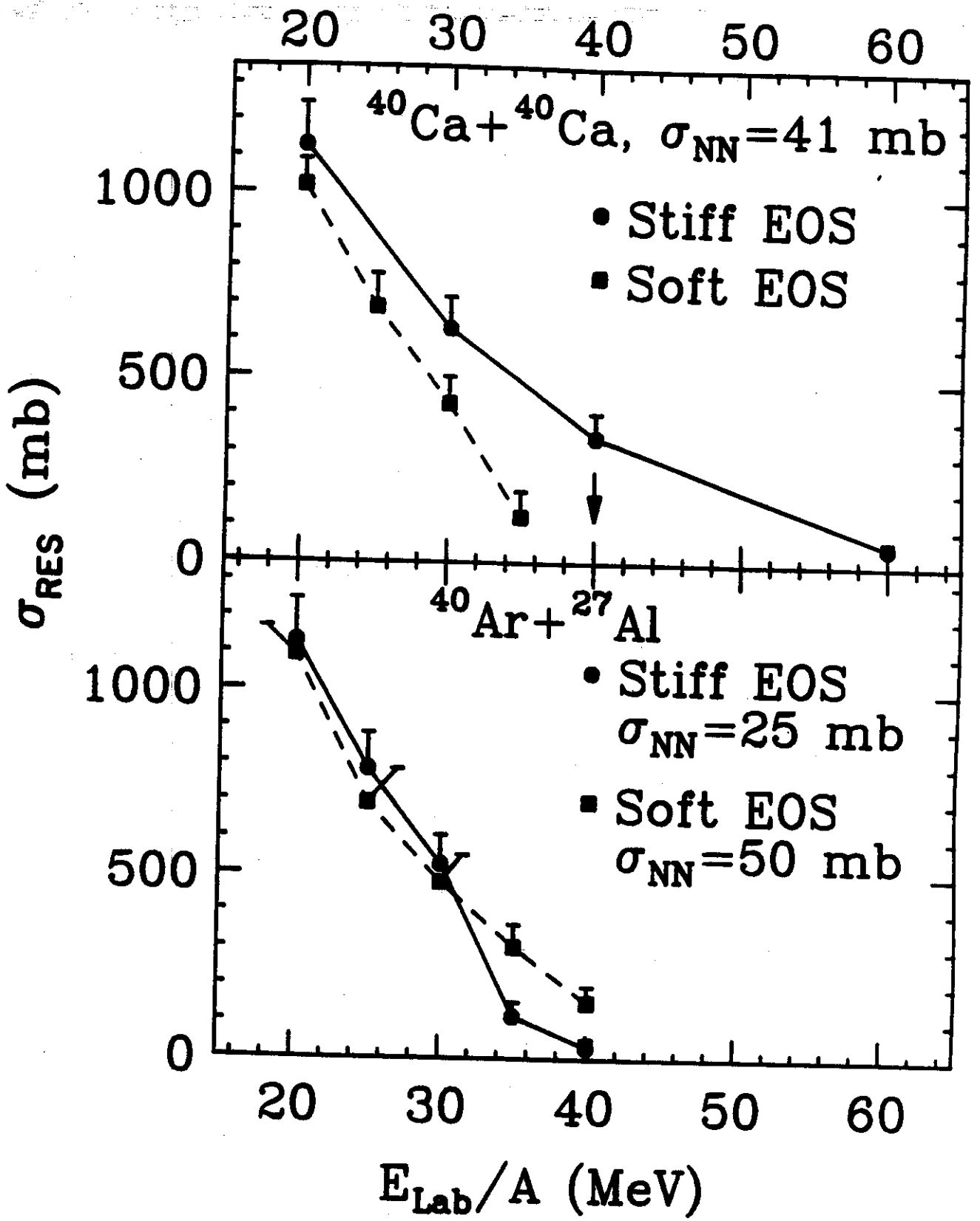
20
30
40
50
60
$^{40}Ca+^{40}Ca$, σ_{NN}=41 mb
• Stiff EOS
▪ Soft EOS
1000
500
0
σ_{RES} (mb)
$^{40}Ar+^{27}Al$
• Stiff EOS
σ_{NN}=25 mb
▪ Soft EOS
σ_{NN}=50 mb
1000
500
0
20
30
40
50
60
E_{Lab}/A (MeV)

Fig. 2

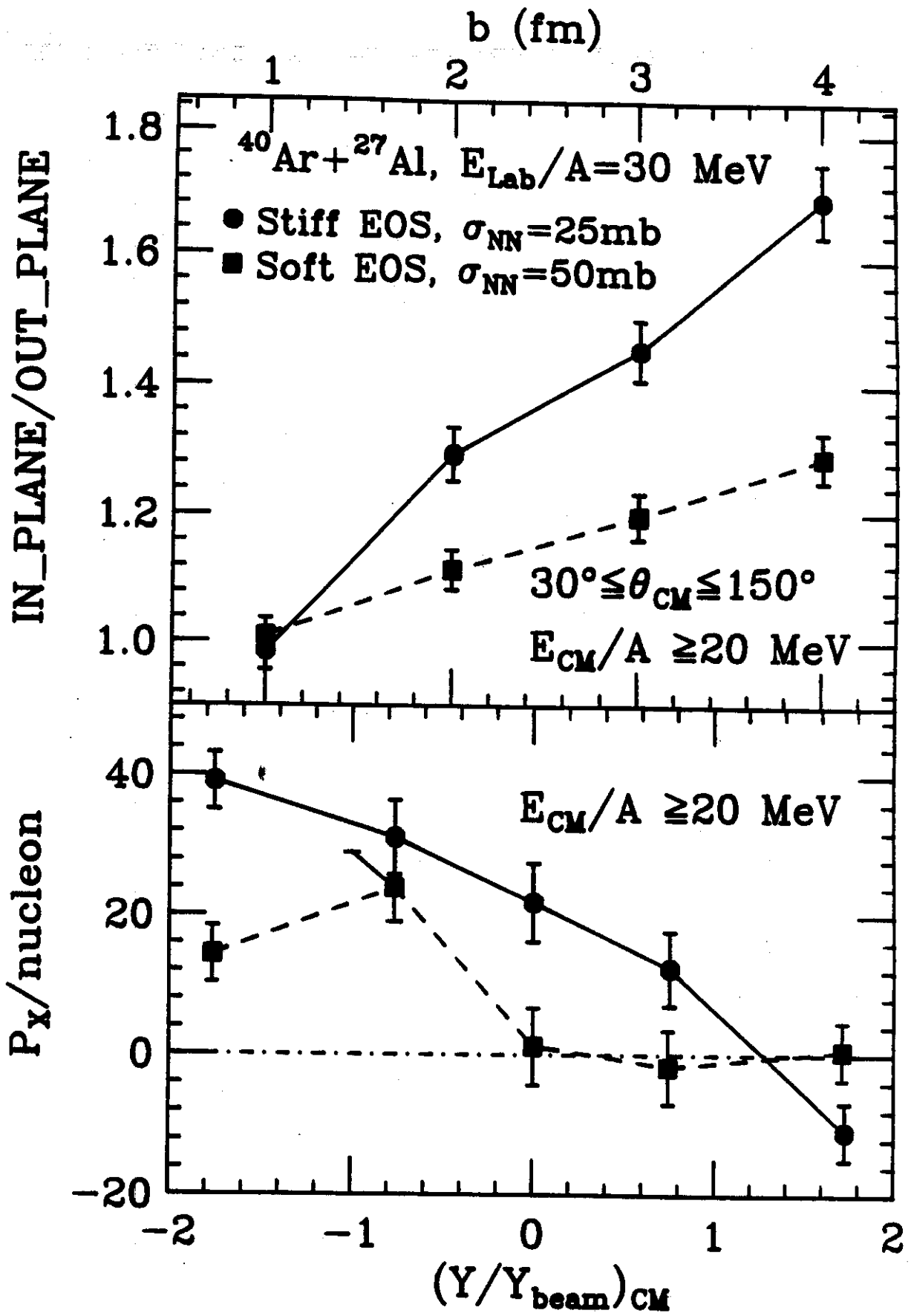
b (fm)
1
2
3
4
1.8
1.6
1.4
1.2
1.0
IN_PLANE/OUT_PLANE
^{40}Ar+^{27}Al, E_{Lab}/A=30 MeV
Stiff EOS, σ_{NN}=25mb
Soft EOS, σ_{NN}=50mb
30°≤θ_{CM}≤150°
E_{CM}/A ≥20 MeV
40
20
0
−20
P_x/nucleon
E_{CM}/A ≥20 MeV
−2
−1
0
1
2
$(Y/Y_{beam})_{CM}$

Fig. 3